

# A 2.5MHz Bandpass Active Complex Filter with 2.4MHz Bandwidth for Wireless Communications

A. Villegas, R. Bianca, A. Ginés, R. Doldán, M.A. Jalón, A.J. Acosta, E. Peralías, D. Vázquez and A. Rueda

Instituto de Microelectrónica de Sevilla - Centro Nacional de Microelectrónica  
Consejo Superior de Investigaciones Científicas (IMSE-CNM-CSIC) / Universidad de Sevilla  
Avda Reina Mercedes s/n – Edificio CICA-CNM - 41012 – Sevilla - Spain  
Email: villegas@imse.cnm.es

*Abstract— This paper presents a fully differential 8<sup>th</sup>-order transconductor-based active complex filter with 2.4MHz bandwidth and centered at 2.5MHz, designed in a 90nm 2.5V 7M and MIM capacitors CMOS process technology. The filter compliants with the requirements of the IEEE802.15.4 standard. Simulation results including mismatching and process variations over the extracted view of the circuit are shown. The filter has a nominal gain of 12dB, good selectivity (20dB@2MHz offset), high image rejection (51dB nominal) and low power consumption (3.6mA @2.5V).*

## I. INTRODUCTION

At present, Low-IF architectures are used in most of modern RF transceivers because they combine the advantages of both IF and zero-IF (or direct-conversion) topologies [1] while maintain a good compromise in terms of power dissipation, integration capability and complexity. Indeed, they down-convert the desired channel placed above the flicker noise corner avoiding the DC offsets and  $1/f$  noise. However, the image problem arises in this kind of architecture [1]. As shown in Figure 1, the action of mixing not only converts-down (to  $\omega_{IF}$ ) the desired band ( $\omega_{LO} + \omega_{IF}$ ) but also the image band placed symmetrically ( $\omega_{LO} - \omega_{IF}$ ) with respect the multiplying frequency ( $\omega_{LO}$ ). So, both the desired and

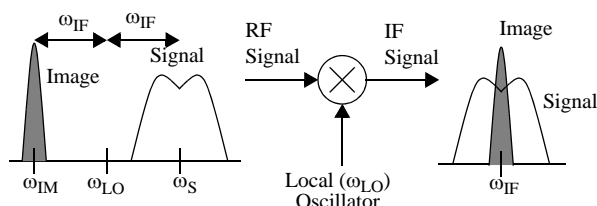


Figure 1 :Image problem in Low-IF receivers.

the image band (that can have even higher power than the desired band) are superimposed in the same output band.

A way to overcome the image problem consists on attenuating any signal present at the image band prior the mixing operation using a passive RF filter [2] [3]. However, this solution is very difficult due to the sensitivity to process variations and parasitic effects. The solution contemplated in this paper, widely accepted, is based on the use of complex or polyphase filters as shown in the Low-IF architecture with quadrature down-conversion in Figure 2 [4] - [7]. The RF signal is amplified and down-converted to IF with two mixers in quadrature. Channel selection and image rejection is performed by a complex filter.

This paper presents an 8<sup>th</sup>-order transconductor-based active complex filter with 2.4MHz bandwidth and centred at 2.5MHz designed in a 90nm 2.5V CMOS technology compliant with the requirements imposed in the IEEE802.15.4 [8]. The paper is organized as follows. Section II reviews the principles of complex filters. Section III describes the filter synthesis and design of building blocks accordingly to the specifications. Simulation results are presented in Section IV. Finally, conclusions are given in Section V.

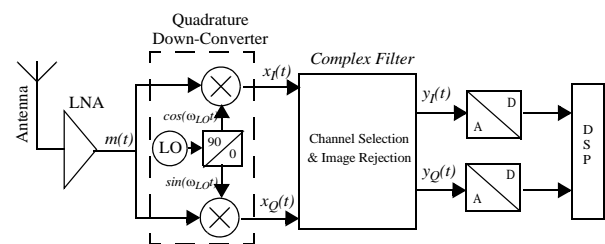


Figure 2 :Typical Low-IF architecture with quadrature down-conversion

## II. BASIS OF COMPLEX FILTERS

For an RF signal  $m(t)$  with the spectrum shown in Figure 3a, the corresponding spectrum of the quadrature down-converted complex signal  $x_C(t)$  composed as,

$$x_C(t) = x_I(t) + jx_Q(t) = m(t)e^{j\omega_{LO}t} \quad (1)$$

results as shown in Figure 3b. As can be seen, the wanted band is on the positive frequencies while the image band is in the negative ones. To eliminate the image, it is necessary to filter out the signal with a filter able to discriminate between positive and negative frequencies like a complex filter do. A matched filter can be conveniently designed to perform the channel selection (pass the signal band) while rejecting the image to give a filtered complex signal  $y_C(t) = y_I(t) + jy_Q(t)$  with the spectrum shown in Figure 3c.

The complex filter in Figure 2 has two inputs ( $x_I$  and  $x_Q$ ) and two outputs ( $y_I$  and  $y_Q$ ). So, the filter is characterized by four transfer functions (all possible combinations between inputs and outputs). The required filter needs to implement a bandpass transfer function centred at positive frequencies (namely  $\omega_{IF}$ ), while

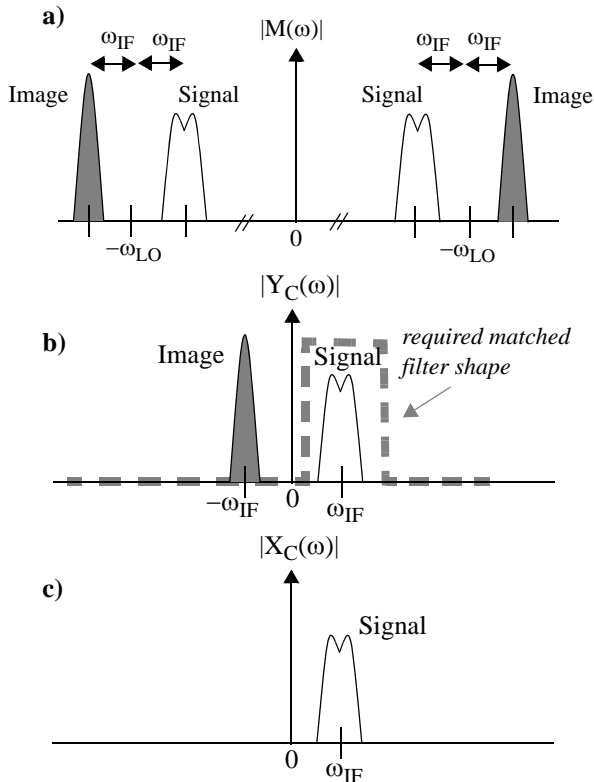


Figure 3 :Spectrum of complex signals in the architecture of Figure 2. a) RF signal before mixing, b) IF signal after mixing. c) IF signal after filtering.

negative frequencies should be rejected. The transfer function of such a filter can be obtained from a lowpass prototype with real coefficients, as illustrated in Figure 4, by performing a proper linear frequency shifting of poles (Figure 4a). This way, the shape of the lowpass prototype is also maintained. Figure 4b shows the block diagram of the implementation for a first order section. Higher order sections can be realized by applying the same strategy to any integrator

## III. PROPOSED COMPLEX FILTER

The complex filter to be designed is intended for wireless communications compliant with the specifications of the IEEE.802.15.4 standard in the 2.4GHz band [8]. It imposes a channel bandwidth of 2MHz, 0dB in the adjacent and -30dB attenuation in the alternative channels (image band is considered in this case) with respect to the channel band. Moreover, the standard also dictates that the system should work properly in the presence of a frequency offset of 200kHz.

At first, the selection of the IF frequency is of main concern. A good compromise widely accepted in terms of practical realization and power consumption is to use an IF frequency equal (or slightly larger) the channel bandwidth. This way, and in order to cope with the

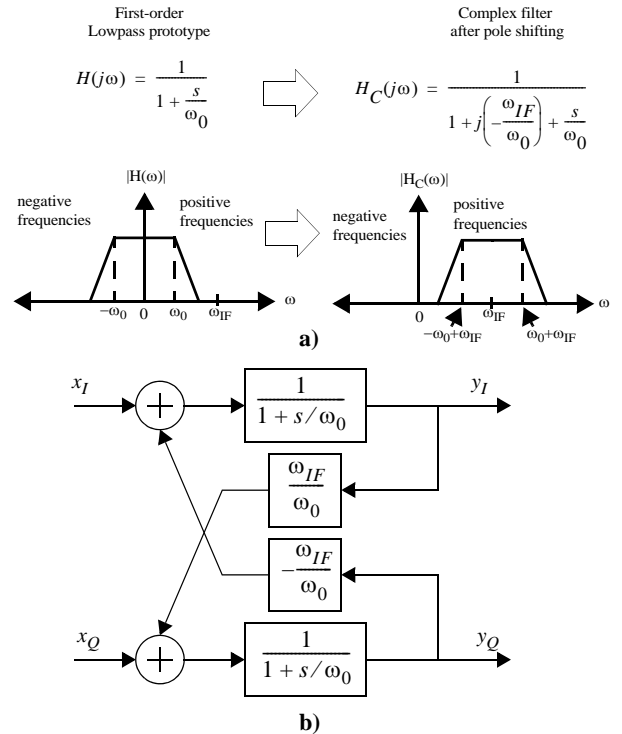


Figure 4 :a) Illustration of pole shifting in the complex domain. b) Implementation block diagram of a first order section.

specified channel bandwidth of 2MHz and the frequency offset of 200kHz, a 2.5MHz IF and a channel bandwidth of 2.4MHz have been set for the filter to be synthesized.

### A. Lowpass filter prototype

As described previously, the complex filter can be derived from a lowpass prototype by substituting the real integrators by complex ones. Then, the lowpass prototype should exhibit a bandwidth of 1.2MHz, and an attenuation of -30dB at 7.5MHz (alternative channel).

It can be shown that a fourth-order all pole transfer function with the poles location and quality factors in Table I accomplishes with the needs with certain security margins. The corresponding normalized magnitude response is in Figure 5. Table II shows the resulting selectivity characteristics of the filter.

Poles location	Quality factor
0.9471MHz	0.6188
1.3839MHz	2.1829

Table I: Complex poles location and quality factors of the synthesized lowpass prototype.

Channel Band	Frequency Band	Attenuation
Passband Ripple	0 - 1.2MHz	0.1dB
Transition Band	1.2MHz-2.5MHz	--
Adjacent Channel	2.5MHz-7.5MHz	10dB
Alternative Channels	>7.5MHz	40dB

Table II: Selectivity characteristics of the synthesized lowpass prototype.

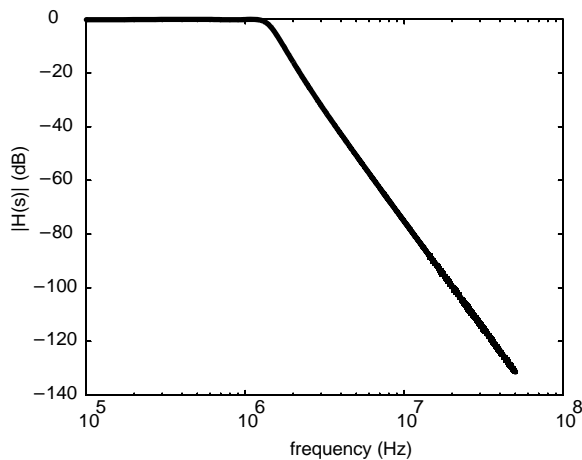


Figure 5 :LPF normalized magnitude response.

### B. Complex filter implementation

Among other implementation techniques (passive RC, MOSFET-C, etc.), the  $G_m$ -C style has been chosen to implement the filter. The reasons are several: possibility to provide gain and reduce noise effects, good trade-off in terms of power and operating frequency, etc. Moreover, the relatively low quality factor of poles (Table I) allows to avoid Q-tuning and simplify the final design [9]-[10].

The filter has been built as a cascade of second-order transfer functions using the basic structure in Figure 6a. Sections have been ordered in increasing order of pole quality factor to optimize the dynamic range and a gain of 12dB has been set to the first section. Table III shows the required parameters value. Finally, transforming the lowpass prototype to its bandpass complex counterpart requires two crossing extra signal paths per integrator. The resulting architecture is in Figure 6b, while the values of the crossing transconductors are in Table IV.

Section #	$G_{m1}$ ( $\mu A/V$ )	$G_{m2}$ ( $\mu A/V$ )	$G_{m3}$ ( $\mu A/V$ )	$G_{m4}$ ( $\mu A/V$ )	$C_1$ (pF)	$C_2$ (pF)
1	200	100	50	50	10.3	10.3
2	10	50	100	100	12.5	10.5

Table III: Parameters value for the lowpass filter.

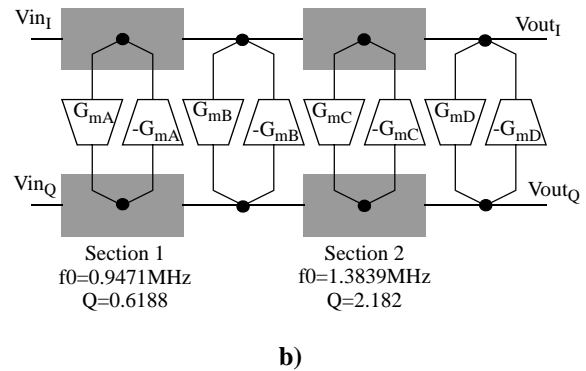
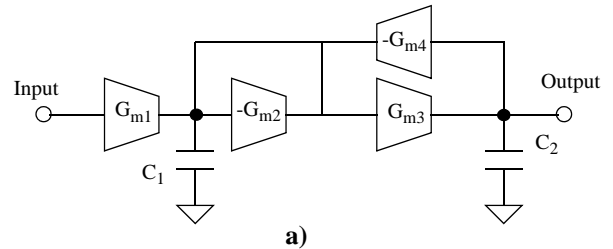


Figure 6 :Filter diagram blocks. a) Lowpass 2nd-order structure. b) Complex filter implementation

$G_{m_A}$ ( $\mu A/V$ )	$G_{m_B}$ ( $\mu A/V$ )	$G_{m_C}$ ( $\mu A/V$ )	$G_{m_D}$ ( $\mu A/V$ )
163.2	197.3	106.6	165.4

Table IV: Parameters value of complex transconductors

### C. Building blocks

A fully differential implementation of the filter has been designed and integrated in a 90nm 2.5V 7metal layers and MIM capacitors ( $2fF/\mu m^2$ ) CMOS process. Figure 7 shows the schematic of the basic transconductor. It is a source degenerated transconductor where cascode transistors (M5-M8) have been added to improve the output impedance. It can be shown that the effective transconductance ( $G_m$ ) is given by [10],

$$G_m = \frac{g_m}{1 + g_m R} \quad (2)$$

where  $g_m$  is the transconductance of the input transistors (M1-M2), and  $R$  is the equivalent resistance of transistor  $M_{res}$ . So,  $G_m$  can be easily tuned through  $M_{res}$  gate voltage  $V_c$ . The common mode feedback circuitry consists on a pair of coupled differential pairs and has been sized to stabilize the common mode level around 1.1V. A unitary transconductor of  $50\mu A/V$  has been designed. This way, and for matching considerations, all the transconductors in the lowpass filter are built by connecting in parallel the necessary units. The crossing transconductors ( $G_{m_A}$  to  $G_{m_D}$ ) are built by an integer number of unitary elements plus an extra element (in fact, the unitary transconductor slightly modified) to adjust the required transconductance value. Capacitors are built in the same manner using a unitary element of 1.7pF.

## IV. RESULTS

Several Spectre simulations of the extracted view of the circuit have been carried out.

Figure 8 shows the layout of the unitary transconductor. Its size is  $51.4\mu m \times 27.6\mu m$  approximately. Figure 9 depicts the input/output characteristic. The tuning range of the transconductance is around 20% with respect to the nominal case, what is enough to tune the complete filter.

Figure 10 shows the layout of the complex filter, which occupies and area of  $672 \times 540 \mu m^2$  approximately. Routing has been done with extreme care to avoid unbalance between the differential and complex signal paths. The magnitude response of the complex filter under nominal process conditions and temperature is in

Figure 11. In order to ensure proper frequency tuning, channel selection and image rejection under different process and temperature conditions, a Montecarlo analysis including component mismatching has been carried out. Figure 12 shows the resulting responses after frequency tuning; the image rejection in the worst case is 33dB. The output noise power spectral density (Figure 13) at 2.5MHz is  $170nV/\sqrt{Hz}$ , while the integrated noise in a 2MHz band is  $252\mu V_{rms}$ . The third order intermodulation (IIP3) has been measured with two tones at 2.5MHz and 1.5MHz, obtaining 3.2dBm. The 1dB Compression Point is 0.4dBm. The overall performance of the filter is summarized and compared with other reported approaches in Table V.

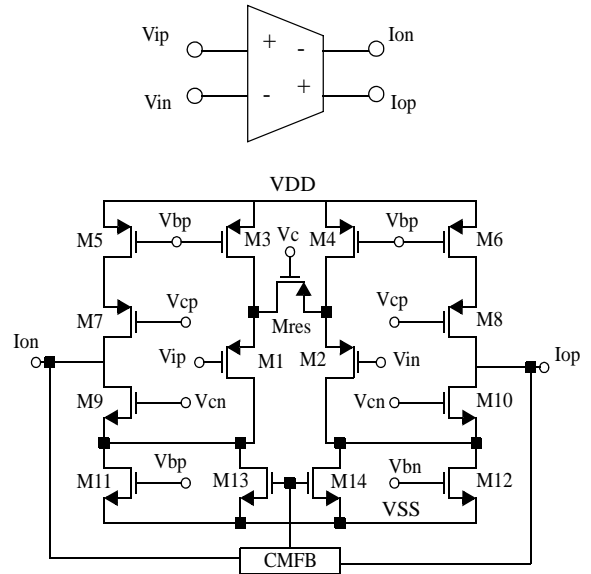


Figure 7 :Transistor level schematic of the basic fully-differential transconductor.

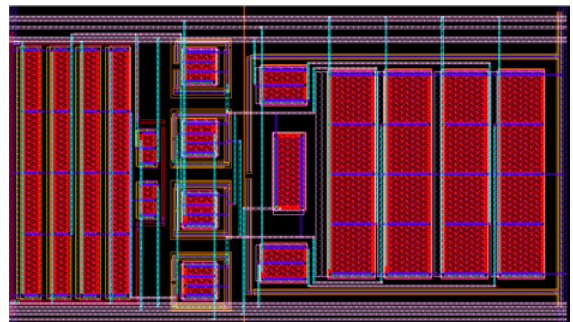


Figure 8 :Layout of the unitary transconductor of value  $50\mu A/V$ .

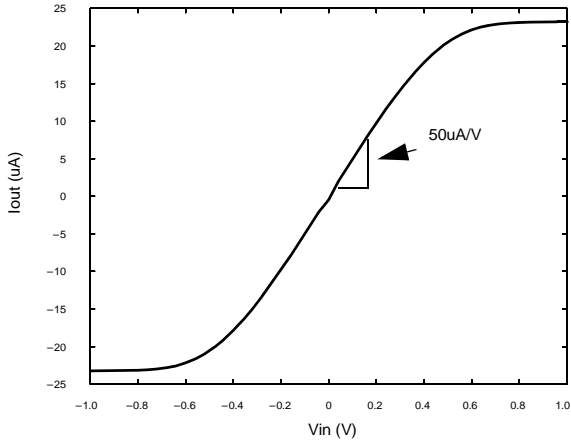


Figure 9 :Input/output characteristic of the unitary transistor of value 50uA/V.

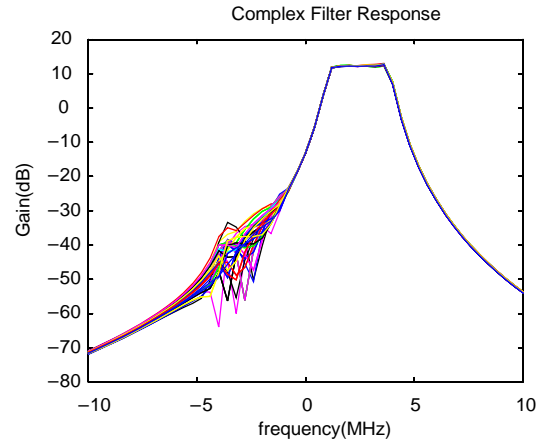


Figure 12 :Magnitude response of the filter under different process and temperature conditions.

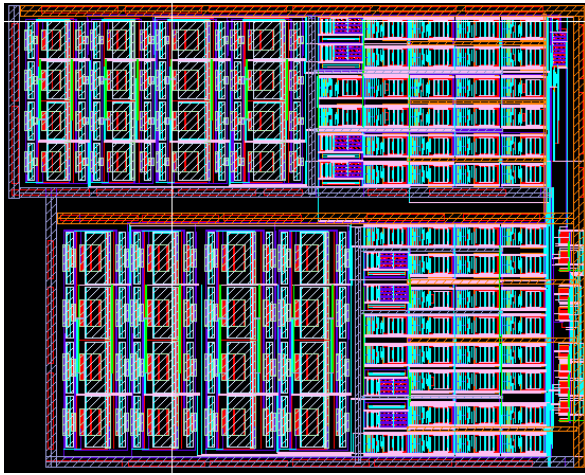


Figure 10 :Layout of the designed complex filter.  
Size is 672x540  $\mu\text{m}^2$ .

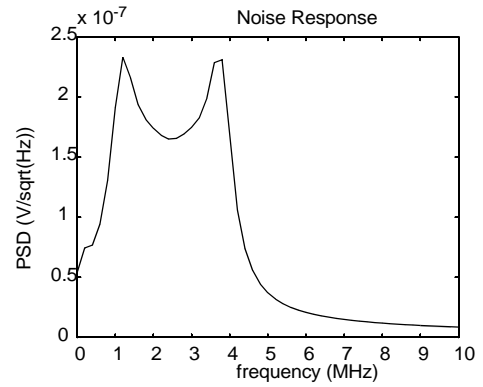


Figure 13 :Output Power Spectral Density.

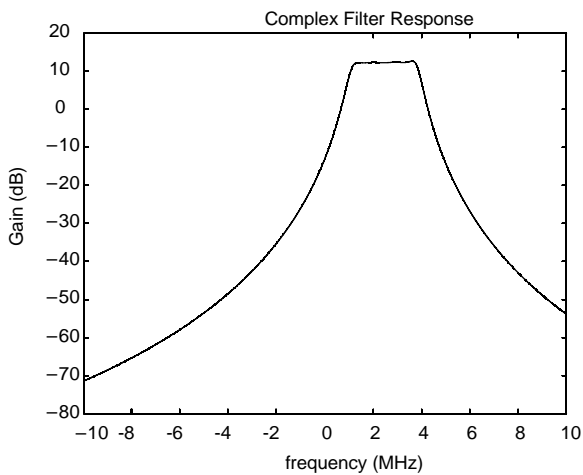


Figure 11 :Magnitude response of the complex filter under nominal conditions.

	<b>This work</b>	[5]	[6]	[7]
Filter order	8	8	10	8
Filter Ripple (dB)	0.1	0.5	0.5	-
Supply Voltage (V)	2.5	2.5	1.8	2.7
Minimum Transistor Channel Length ( $\mu\text{m}$ )	0.28	0.6	0.18	0.35
Supply Current (mA)	3.6	2.4	1.38	4.7
Centre Frequency (MHz)	2.5	3	2	2
Bandwidth (MHz)	2.4	0.97	2.4	1
Gain (dB)	12	0	-6.2	15
Output integrated noise ( $\mu\text{V}_{\text{rms}}$ @MHz)	252@2	250@1	374@2	163@1
1 dB Comp. point (dBm)	0.4	-	-	-
3 <sup>rd</sup> Order Intercept - IIP3 (dBm)	3.2	-	-	-
Image-band rejection (IBR) (dB)	51	53	56	45

Table V: Summarized nominal performance of the designed filter compared with other reported solutions.

## V. CONCLUSIONS

This paper presents a fully differential 8<sup>th</sup>-order transconductor-based active complex filter with 2.4MHz bandwidth and centered at 2.5MHz, designed in a 90nm 2.5V 7metal layers and MIM capacitors CMOS process technology, compliant with the requirements of the IEEE802.15.4 standard. Simulation results including mismatching and process variations over the extracted view of the circuit have been shown. The filter has a nominal gain of 12dB, good selectivity (20dB@2MHz offset), high image rejection (51dB) and low power consumption (3.6mA @2.5V).

## ACKNOWLEDGMENT

This work has been founded in part by the EC through the project A109-Medea+ WITNESS (Wireless technologies for small area networks with embedded security and safety), the Spanish Regional Government of Junta de Andalucía under project TIC-927 and the Spanish Government under project TEC2007-68072.

## VI. REFERENCES

- [1] B.Razavi, "RF Microelectronics". Englewood Clifff, NJ: Prentice-Hall, 1998.
- [2] W.Kluge et al.: "A Fully Integrated 2.4GHz IEEE802.15.4 Compliant Transceiver for ZigBee Applications", IEEE Int. Jour. of Solid-State Circuits, Vol. 41, N 12, pp. 2767-2775, 2006.
- [3] F.Haddad et al.: "Radio Frequency polyphase filter design in 0.13um CMOS for wireless communications", in Proc. of IEEE Int. Workshop on Radio-Frequency Integration Technology (RFIT2007), pp. 175-178, Dec. 2007, Singapore.
- [4] F. Behbahani, Y. Kishigami, J. Leete, and A. A. Abidi, "CMOS mixers and polyphase filters for large image rejection," IEEE J. Solid-State Circuits, vol. 36, pp. 873–887, June 2001.
- [5] P. Andreani and S. Mattison, "A CMOS gm-C IF Filter for Bluetooth", IEEE 2000 Custom integrated circuits conference, pp 391-394.
- [6] P. Khumsat and A. Worapishet, "Design of 1.8-V CMOS Polyphase Filter for Dual-Mode Bluetooth/ZigBee Transceiver", ECTI transactions on electrical Eng. Electronics and communications vol.4 no. 1, pp. 29-34, February 2006.
- [7] A. A. Emira and E. Sánchez-Sinencio, "A Pseudo Differential Complex Filter for Bluetooth With Frequency Tuning", IEEE transactions on circuits and systems II: Analog and Digital Signal Processing, vol. 50, no. 10, pp. 742-754, October 2003.
- [8] Wireless Medium Access control (MAC) and Physical Layer (PHY) Specifications for Low-Rate Wireless Personal Area Network (LR-WPANs), IEEE 802.15.4, October 2003.
- [9] R.Schaumann, M.D. Ghousi and K.R. Laker, "Design of Analog Filters", Prentice Hall Communications Engineering Emerging Technologies Series.
- [10] J. E. Kardontchik, "Introduction to the design of Transconductor-Capacitor Filters", Kluwer Academic Publications, 1992.